

# REQIBA: Regression and Deep Q-Learning for Intelligent UAV Cellular User to Base Station Association

Boris Galkin\*, Erika Fonseca\*, Ramy Amer\*, Luiz A. DaSilva\*<sup>†</sup>, and Ivana Dusparic\*

\* CONNECT- Trinity College Dublin, Ireland

<sup>†</sup> Commonwealth Cyber Initiative, Virginia Tech, USA

E-mail: {galkinb,fonsecae,ramyr,duspari}@tcd.ie, ldasilva@vt.edu

**Abstract**—Unmanned Aerial Vehicles (UAVs) are emerging as important users of next-generation cellular networks. By operating in the sky, these UAV users experience very different radio conditions than terrestrial users, due to factors such as strong Line-of-Sight (LoS) channels (and interference) and Base Station (BS) antenna misalignment. The consequence of this is that the UAVs experience significant degradation to their received quality of service, particularly when they are moving and are subject to frequent handovers. The solution is to allow the UAV to be aware of its surrounding environment, and intelligently connect into the cellular network using this awareness. In this paper we present REgression and deep Q-learning for Intelligent UAV cellular user to Base station Association (REQIBA) to allow a UAV which is flying over an urban area to intelligently connect to underlying BSs, using information about the received signal powers, the BS locations, and the surrounding building topology. We demonstrate how REQIBA can as much as double the total UAV throughput, when compared to heuristic association schemes similar to those commonly used by terrestrial users. We also evaluate how environmental factors such as UAV height, building density, and throughput loss due to handovers impact the performance of our solution.

**Index Terms**—Cellular-connected UAVs, Machine Learning, Reinforcement Learning.

## I. INTRODUCTION

Unmanned Aerial Vehicles (UAVs) are a new type of aircraft that operate without a pilot on board. Instead, they are either piloted remotely by a human operator, or they are controlled by computer algorithms. These devices are becoming increasingly used in a variety of applications, such as medical deliveries [1], building inspections, and surveillance [2]. To enable these applications, the UAVs will require a reliable wireless data link with their pilot or other controlling entities. While current commercially-available UAVs rely on direct connections to their pilot, there is growing interest in connecting the UAVs via cellular networks [3], [4], [5]. The emerging Fifth Generation (5G) family of cellular standards is intended to accommodate new types of users which require very high levels of reliability; this makes the 5G network an attractive option for facilitating UAV connectivity [6].

Until very recently, the cellular network was exclusively used by devices operating at – or close to – ground level. Existing cellular networks were designed with these users in

mind, with Base Station (BS) locations chosen to create coverage “cells” for the ground users, and the antennas configured to transmit signals towards the ground. Because they operate in the sky, UAVs experience very different radio conditions to those of ground users, and the design of existing cellular networks introduces significant issues for them [3]. Experimental trials have shown that while flying, UAVs are likely to receive sidelobe signals from the BSs, as the mainlobes are aimed towards the ground [7]. The sidelobe signal gain may be such that a UAV may receive a stronger signal from a BS which is kilometers away from it than from a BS which is closer. Furthermore, a UAV is able to establish unobstructed Line-of-Sight (LoS) channels to a large number of BSs. The consequence of this is that, while at ground level the network may be partitioned into coverage “cells”, at greater heights the network coverage is highly volatile, with very strong interference from distant BSs and a large number of BSs that a UAV can connect to at any given moment [8].

As a result of this, a UAV travelling through an area is likely to see very rapid signal fluctuations, and may potentially hand off from one BS to another very frequently. These frequent handovers may introduce significant overheads into the network performance, and degrade the service quality for the UAV link. The 3rd generation partnership project (3GPP) has suggested that steerable, directional antennas should be used by the UAVs, as they can allow a UAV to improve its wireless link quality by reducing the power of undesirable BS signals (i.e. interference) [3]. As the UAVs are capable of intelligent movement a number of works have suggested that UAVs should optimise their flight trajectories with respect to the underlying cellular network, to improve performance. A variety of algorithms have been proposed for this trajectory optimisation, as discussed in the next section. While this type of optimisation is useful for scenarios where the UAV trajectory can be optimised with respect to cellular service, there are a variety of scenarios where the trajectory of the UAV may not be modified, either because the flight path is explicitly defined by the UAV mission (such as photography work) or because the UAV is being piloted in real-time by a human operator rather than a computer algorithm. In these scenarios, the UAV can improve its service quality and manage its handover rate by intelligently choosing which BSs to associate

with, using knowledge of its surrounding environment. When equipped with a steerable directional antenna, this would allow the UAV to align its antenna to create the best wireless channel for the given circumstances.

In our prior work [9] we addressed the issue of intelligent UAV-BS association in a static scenario where the UAV was hovering in place and needed to make a single association decision for its location. While our proposed neural network solution was shown to outperform conventional association schemes in terms of channel quality, as the scenario was static we did not address the issue of UAV movement and the resulting handovers. In this paper we extend our prior work by considering a scenario where a UAV needs to intelligently maintain a connection to the underlying cellular network while moving, by making multiple association decisions during flight. Our contributions are stated as follows:

- We propose a neural network-based solution which we refer to as REgression and deep Q-learning for Intelligent UAV cellular user to Base station Association (REQIBA), which allows a UAV equipped with a directional antenna to intelligently associate with nearby BSs during flight. This solution consists of a regression neural network and a Dueling Deep Q-Network (DDQN) module. The solution takes in state information about the environment, information about received signal power, interference, and current BS connection. The network then chooses a BS to connect to based on these factors, to maximise the data throughput.
- We evaluate the performance of our REQIBA solution, to demonstrate that addressing this problem in a mobility scenario is indeed a lot more complex than treating it as a series of static connection decisions. We demonstrate how REQIBA outperforms our prior solution in [9] by simultaneously increasing the total throughput and reducing the rate of UAV handovers.
- We compare the performance of REQIBA against heuristic association schemes. We demonstrate how it outperforms these heuristic schemes under different environmental conditions, while exploring how these environmental conditions affect its performance improvement.

This paper is structured as follows. In Section II we review the related works. In Section III we outline our system model. In Section IV we introduce and describe our REQIBA solution. In Section V we describe how REQIBA is trained and evaluated. In Section VI we compare the performance of REQIBA against our prior solution in [9]. In Section VII we evaluate how REQIBA performs against the heuristic algorithms under various environmental conditions. Finally, in Section VIII we provide our conclusions and discuss directions for further investigation.

## II. RELATED WORKS

The cellular connectivity issues experienced by flying UAVs have been extensively explored. In [10] Qualcomm reports the results of a series of simulations and field measurements which determine that UAVs are exposed to stronger interference than ground users. In [11] the authors apply stochastic geometry

to demonstrate how UAVs experience throughput degradation with increasing heights, due to growing interference power. In [12], [13] the authors use simulations to show how UAVs experience very high handover failure rates due to strong interference conditions at large heights. In [14], authors perform an experimental flight with a UAV at different heights and speeds, and conclude that a UAV performs approximately 5 times more handovers than ground users moving at the same speed. In our prior work [15] we demonstrate how BS sidelobes can cause frequent UAV handovers during UAV vertical movement.

As UAVs are highly mobile devices, the wireless community typically approaches the problem of UAV cellular connectivity from the perspective of optimising the UAV trajectory. In [16] the authors consider a UAV that needs to fly between two locations, in a manner that minimises the flight time while maintaining a reliable cellular link. They use a graph representation of the network and apply Dijkstra's algorithm to find the route of the UAV. The authors of [17] optimise the movement of a UAV around a map of LoS-blocking buildings, to ensure the UAV maintains a LoS channel to its BS. A similar work is carried out in [18], where UAV relays are intelligently positioned around known user locations as well as the locations of buildings. In [19] the authors optimise the UAV trajectory given available landing sites where the UAV can land and reduce its energy consumption. As there is significant research interest in the UAV trajectory optimisation topic, machine learning (ML) is seeing widespread application in the UAV domain. In [20], authors investigate interference-aware trajectory optimisation using game-theory and ML for the purpose of maximizing energy efficiency and minimizing wireless latency and the UAV interference on the ground network. Authors in [21] propose an ML approach to find an optimal trajectory which minimizes the travel time while maintaining connectivity with the cellular network. Meanwhile, the work in [22] proposes a deep learning-based framework to manage the dynamic movement of multiple UAVs in response to ground user mobility so as to maximize the sum data rate of the ground users.

Along with the ongoing work on UAV trajectory optimisation, the wireless community is also beginning to address the issues associated with UAV handovers using ML tools. For instance, the authors in [23] show how ML can be used to dynamically adjust the BS antenna tilt angles. The authors apply model-free Reinforcement Learning (RL) to the BS antenna tilt such that the agent balances the received signal power for a UAV user passing overhead with the throughput of the ground users. The authors demonstrate how this intelligent antenna tilting can help reduce the UAV handover rate without significant performance loss for the ground users. In [24], the authors consider a joint BS selection and resource allocation problem for moving UAVs. The authors apply reinforcement learning to simultaneously select the serving BS and the allocated resource blocks with the aim of minimizing the uplink interference created by the UAV for the ground users, while keeping the rate of UAV handovers manageable. A similar problem is addressed in [25], where the authors intelligently select BS associations for a UAV moving along a known trajectory to minimise the rate of handovers. In [26], the

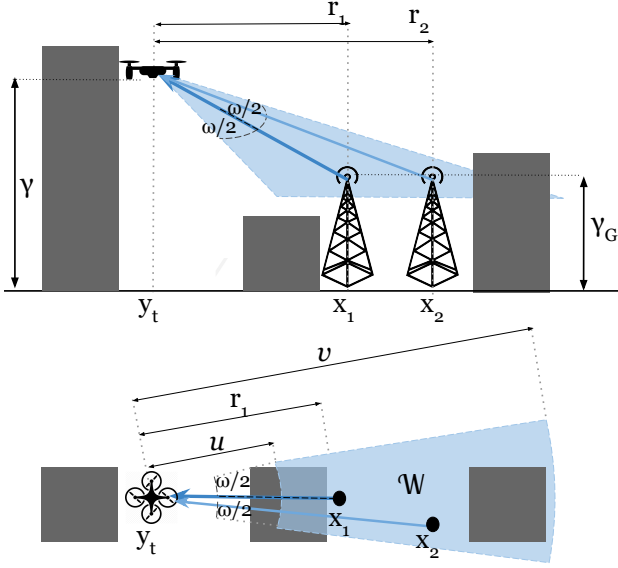


Fig. 1. Side and top view showing a UAV in an urban environment at a height  $\gamma$ , positioned above  $y_t$  with antenna beamwidth  $\omega$ . The UAV chooses to associate with the BS at  $x_1$  and centers its antenna main lobe on the BS location; the blue area  $\mathcal{W}$  illuminated by the main lobe denotes the region where interferers may be found. The BS at  $x_2$  falls inside this area and produces interference.

authors envision a method for managing a UAV flight path to coordinate enhanced handover in 3GPP networks. In our prior work [9], we consider the problem of UAV association, where the UAV is equipped with a directional antenna for communication, and an omni-directional antenna for sensing. Our proposed ML solution in that paper uses the available channel information from the omni-directional antenna as well as the known locations of the interfering BSs to infer which BS will exhibit the best channel conditions for the directional antenna.

This work extends our prior work in [9]. While our prior work considers optimising the channel quality in a scenario where a UAV is hovering at a fixed location, in this work we consider a moving UAV. This movement introduces the issue of UAV handovers, which complicates the association problem and requires an entirely new ML solution. Note that our work differs from existing works such as [24] and [25] in that we consider a throughput-maximisation problem for a UAV which communicates via a steerable directional antenna rather than an omni-directional one. This complicates the process of gathering environmental information for the association decision, which requires us to use a more complex ML solution to successfully optimise the UAV performance, as we will demonstrate in later sections.

### III. SYSTEM MODEL

We consider an urban environment where a flying UAV uses an underlying cellular network for its wireless connectivity, as depicted in Fig. 1. The underlying cellular network consists of BSs which are horizontally distributed as a homogeneous Poisson point process (PPP)  $\Phi = \{x_1, x_2, \dots\} \subset \mathbb{R}^2$  of intensity  $\lambda$ , at a height  $\gamma_G$  above ground. Elements  $x_i \in \mathbb{R}^2$  represent the projections of the BS locations onto the  $\mathbb{R}^2$  plane.

The UAV travels from an initial location  $y_1 \in \mathbb{R}^2$  to a final location  $y_T \in \mathbb{R}^2$  in a straight line over a length of time  $T$ . We discretise time into  $T$  timesteps: this lets us partition the travel vector of the UAV into  $T$  coordinates at different timesteps in the journey. We define the vector of these UAV coordinates as  $\mathbf{u} = (y_1, y_2, \dots, y_t, \dots, y_T)$ , where  $y_t$  denotes the coordinates of the UAV in the  $t$ -th timestep. The UAV height above ground remains constant throughout the flight and is denoted as  $\gamma$ . Let  $r_i^t = \|x_i - y_t\|$  denote the horizontal distance between the coordinates  $x_i$  and  $y_t$ , and let  $\phi_i^t = \arctan(\Delta\gamma/r_i^t)$  denote the vertical angle, where  $\Delta\gamma = \gamma - \gamma_G$ .

The UAV is equipped with two sets of antennas: an omni-directional antenna for BS pilot signal detection and signal strength measurement, as well as a directional antenna for communicating with the UAV's associated BS. The omni-directional antenna has an omni-directional radiation pattern with an antenna gain of 1, while the directional antenna has a horizontal and vertical beamwidth  $\omega$  and a rectangular radiation pattern; using the antenna radiation model in [27], the antenna gain is given as  $\eta(\omega) = 16\pi/(\omega^2)$  inside of the main lobe and  $\eta(\omega) = 0$  outside. We denote the coordinates of the BS which the UAV is associated with at time  $t$  as  $x_s^t \in \Phi$  and its horizontal distance to the UAV as  $r_s^t$ . Whenever the UAV connects to a BS  $x_s^t$  it aligns its directional antenna towards  $x_s^t$ ; this results in the formation of an antenna radiation pattern around  $x_s^t$  which we denote as  $\mathcal{W} \subset \mathbb{R}^2$ , as depicted in Fig. 1. This area takes the shape of a ring sector of arc angle equal to  $\omega$  and major and minor radii  $v(\gamma, r_s)$  and  $u(\gamma, r_s)$ , respectively, where

$$v(\gamma, r_s) = \begin{cases} \frac{|\Delta\gamma|}{\tan(|\phi_s^t| - \omega/2)} & \text{if } \omega/2 < |\phi_s^t| < \pi/2 - \omega/2 \\ \frac{|\Delta\gamma|}{\tan(\pi/2 - \omega)} & \text{if } |\phi_s^t| > \pi/2 - \omega/2 \\ \infty & \text{otherwise} \end{cases}$$

$$u(\gamma, r_s) = \begin{cases} \frac{|\Delta\gamma|}{\tan(|\phi_s^t| + \omega/2)} & \text{if } |\phi_s^t| < \pi/2 - \omega/2 \\ 0 & \text{otherwise} \end{cases} \quad (1)$$

with  $|\cdot|$  denoting absolute value. The BSs which fall inside the area  $\mathcal{W}$  are denoted by the set  $\Phi_{\mathcal{W}} = \{x \in \Phi : x \in \mathcal{W}\}$ . The BSs in the  $\Phi_{\mathcal{W}}$  are capable of causing interference to the UAV-BS communication link, as their signals may be received by the UAV's directional antenna with non-zero gain.

As we are considering an urban environment, buildings will affect the wireless signals by blocking LoS links. We model these buildings as being distributed in a square grid, following the model proposed by the ITU in [28]. The density of buildings per square kilometer is  $\beta$  and the fraction of the ground area covered by buildings is  $\delta$ . All buildings have the same horizontal dimensions, and each building has a height which is a Rayleigh-distributed random variable with scale parameter  $\kappa$ . The UAV will have an unobstructed LoS channel towards a BS  $i$  at time  $t$  if there exist no buildings which intersect the straight line between  $x_i$  at height  $\gamma_G$  and  $y_t$  at height  $\gamma$ . Otherwise if there is at least one building that intersects this line then the channel is non-Line-of-Sight (NLoS).

We assume that the BSs have tri-sector antennas, with each antenna being a Uniform Linear Array (ULA) with  $N_t$  antenna elements. For tractability we model these antennas as being horizontally omni-directional with horizontal gain 1. The vertical gain of these antennas is a function of the angle between the UAV and the BS and is defined similar to [29] as

$$\mu(\phi_i^t) = \frac{1}{N_t} \frac{\sin^2 \frac{N_t \pi}{2} \sin(\phi_i^t)}{\sin^2 \frac{\pi}{2} \sin(\phi_i^t)}. \quad (2)$$

When the UAV is connected to the BS at  $x_s$  at timestep  $t$ , the Signal-to-Interference-and-Noise Ratio (SINR) of the signal received by the directional antenna is given as

$$\text{SINR}^t = \frac{p\eta(\omega)\mu(\phi_s^t)c((r_s^t)^2 + \Delta\gamma^2)^{-\alpha_{z_s^t}/2}}{I_L + I_N + \sigma^2} \quad (3)$$

where  $p$  is the BS transmit power,  $\alpha_{z_s^t}$  is the pathloss exponent,  $z_s^t \in \{\text{L}, \text{N}\}$  is an indicator variable which denotes whether the UAV has LoS or NLoS to its serving BS  $x_s$  at timestep  $t$ ,  $c$  is the near-field pathloss,  $\sigma^2$  is the noise power, and  $I_L$  and  $I_N$  are the aggregate LoS and NLoS interference, respectively. The throughput per unit of bandwidth is then given by the Shannon bound as

$$R^t = \log_2(1 + \text{SINR}^t). \quad (4)$$

As already mentioned, we assume that the UAV points its directional antenna at the BS it is currently associated with. The UAV is capable of seamlessly tracking the changing BS orientation using its directional antenna as it moves. If, however, the UAV changes its associated BS in a timestep then the UAV will spend a portion of that timestep realigning its directional antenna towards the new BS. We assume this antenna realignment, along with the handover signalling involved [11], causes an overhead which reduces the effective throughput in that timestep by a factor  $0 \leq \tau \leq 1$  which we refer to as the handover penalty factor. Note that with tri-sector antenna BSs it is possible for a user to handover between two antennas of the same BS; we assume that this type of handover occurs seamlessly and for this reason our focus in this paper is on the handovers between different BSs.

## IV. REQIBA

### A. Problem Statement

The UAV is to fly through the environment from a starting point to an ending point over  $T$  timesteps. At every timestep it is to make a decision about which BS it should be connected to for that timestep. If it decides to connect to a BS other than the one it is currently connected to, it will carry out a handover in that timestep. The reward function for the timestep  $t$  is given as

$$\rho^t = \begin{cases} \log_2(1 + \text{SINR}^t) & \text{if no handover} \\ \tau \log_2(1 + \text{SINR}^t) & \text{otherwise} \end{cases} \quad (5)$$

where  $\tau$  is the handover penalty factor. It follows that the smaller the value of  $\tau$  the less desirable it is for a handover to occur. The optimisation problem consists of maximising the

sum of the throughput across the entire episode of  $T$  timesteps  $\sum_{t=1}^T \rho^t$ . At each timestep the available actions for the UAV consist of the choice of candidate BSs to connect to. In theory the UAV may choose from any BS in  $\Phi$ , but from a practical perspective the choice tends to be limited to only a subset of those BSs. From our prior work [9] we have observed that the UAV is likely to get the best connection from one of the closest BSs to it, or one of the BSs with the strongest received signal power. We therefore denote a subset of BSs  $\Phi_\zeta \subset \Phi$ , where  $\Phi_\zeta$  consists of the  $\zeta/2$  closest BSs to the UAV at timestep  $t$ , as well as the  $\zeta/2$  BSs with the strongest received signal power at the UAV at that timestep. Therefore, at timestep  $t$  the action the UAV takes is to choose from one of the  $\zeta$  candidate BSs in  $\Phi_\zeta$ . Note that the  $i$ -th closest BS at timestep  $t$  may also be the  $j$ -th strongest signal BS where  $i, j \leq \zeta/2$ , which means that the cardinality of set  $\Phi_\zeta$  may be lower than  $\zeta$ .

### B. Available Environmental Information

Before describing our proposed REQIBA solution we specify what state information is assumed to be available to the UAV for use in its decision-making:

- The BS to which the UAV is currently associated.
- The received signal power from nearby BSs. The UAV has an omni-directional antenna for sensing the environment, being able to receive the pilot signals from nearby BSs and determine their received signal power.
- The 3D coordinates of the UAV and the BSs. The UAV knows its location from its Global Positioning System (GPS) coordinates, while the locations of the BSs are provided to it by the network.
- The 3D topology of the environment, as in [18]. To safely navigate through the urban environment we assume the UAV has information on the building locations and heights around it.
- The directional antenna parameters. The UAV is aware of the beamwidth of its directional antenna, and is able to determine the area  $\mathcal{W}$  that would be illuminated by the antenna should it point it at a given location.
- Whether or not it will need to optimise its cellular link in the next timestep. We assume the UAV knows when it no longer needs to continue optimising its cellular connectivity (i.e., the end of the optimisation episode). This information is necessary to tell the learning algorithm whether it should consider future timesteps when choosing an action, or only the current timestep.

While aware of its environment, the UAV does not have complete knowledge of its surroundings. Specifically, the UAV does not know the following:

- The received signal power from all of the individual BSs in the environment. To identify the origin of a received BS signal the UAV needs to be able to decode the pilot signal, which requires the signal to be above a certain minimum SINR threshold.
- Its flight trajectory. For our simulation we assume that the UAV does not know where it is flying, to represent scenarios where the UAV is piloted by a human operator

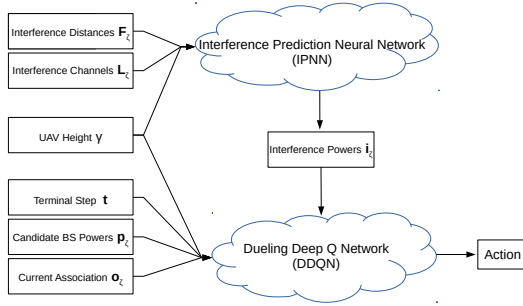


Fig. 2. The structure of our proposed REQIBA solution.

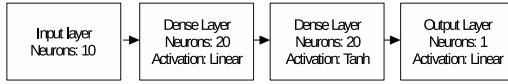


Fig. 3. The IPNN structure.

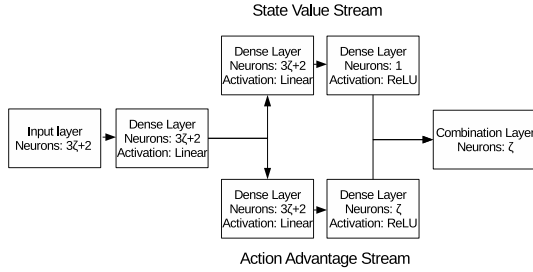


Fig. 4. The DDQN structure.

in real-time rather than following a pre-programmed trajectory.

- Information about future timesteps. As the UAV does not know where it is flying, it does not have any information about future timesteps, such as its own future coordinates.
- BS antenna configuration. We assume that the UAV does not have information about the BS antenna radiation pattern, tilt or transmit power.
- Channel propagation conditions. We assume that the UAV does not know how signals propagate in the environment, nor what the impact of a LoS blockage on the signal is.
- Handover overheads, and the value of  $\tau$ . The UAV does not have prior insight on the performance losses due to handovers, and can only observe the resulting performance after a handover occurs.

### C. REQIBA Solution Structure

It is clear from the reward function in Eq. (5) and the SINR expression in Eq. (3) that the timestep throughput  $\rho^t$  that is obtained after the UAV chooses the BS for that timestep is affected by four factors: whether a handover occurs, the performance penalty of the handover, the received signal power from the associated BS, and the interference power from the other BSs. The UAV explicitly knows before a decision is made whether a handover will occur and the received signal powers from the candidate BSs, and so can use this

information for the decision-making process; however, the handover penalty and the interference powers are not known explicitly. Recall that the omnidirectional antenna that the UAV uses for sensing and the directional antenna used for communication have different radiation patterns, and that the UAV aligns its directional antenna towards its chosen BS, with the interfering BSs coming from the area  $\mathcal{W}$ . The UAV omnidirectional antenna is not able to measure the interference power that comes specifically from the area  $\mathcal{W}$ , this needs to be estimated in some other way. The UAV has access to the map of the BSs, and knows its own directional antenna beamwidth, so it can determine which BSs will fall inside the area  $\mathcal{W}$  and cause interference.

The inputs to our REQIBA solution are as follows. The received signal powers of the  $\zeta$  candidate BSs are provided as a vector  $\mathbf{p}_\zeta = (p_1^t, p_2^t, \dots, p_\zeta^t)$ , where  $p_i^t = p\mu(\phi_i^t)c((r_i^t)^2 + \Delta\gamma^2)^{-\alpha_{z_i^t}/2}$ . The handover information is conveyed with a vector of binary flags  $\mathbf{o}_\zeta = (o_1^t, o_2^t, \dots, o_\zeta^t)$  where  $o_i^t = 1$  if  $x_i^t = x_s^{t-1}$  and 0 otherwise, to indicate which of the candidate BSs the UAV is currently associated with. Information about the interfering BSs consists of two  $\zeta \times \xi$  input matrices  $\mathbf{F}_\zeta$  and  $\mathbf{L}_\zeta$ , where  $\xi$  denotes the number of interfering BSs to consider per link.  $\mathbf{F}_\zeta$  contains the horizontal distances of the interfering BSs to the UAV, where the  $i$ -th row corresponds to the area  $\mathcal{W}_i$  illuminated when the UAV points its directional antenna towards the  $i$ -th candidate BS, and the  $j$ -th column represents the  $j$ -th closest interfering BS in the corresponding illuminated area. The matrix  $\mathbf{L}_\zeta$  contains binary flags to indicate whether the corresponding interfering BSs have LoS or NLoS to the UAV, as determined from the building topology map [18]. If the  $i$ -th candidate BS has less than  $\xi$  interferers then the remaining entries in the  $i$ -th rows of  $\mathbf{F}_\zeta$  and  $\mathbf{L}_\zeta$  take null values. The final two inputs are the UAV height above ground  $\gamma$  and a binary flag  $\mathbf{t}$  which denotes whether the current timestep is the final timestep in the episode.

From Fig. 2 it is clear that the REQIBA solution consists of two separate modules, which are detailed below.

1) *Interference Prediction Neural Network*: Known information about the interference consists of the horizontal distances of the interfering BSs to the UAV and their channel types. To estimate the aggregate interference power using this information, we propose a regression neural network circuit which we refer to as the Interference Prediction Neural Network (IPNN), shown in Fig. 3. This IPNN is trained to estimate the received power from a BS given a known horizontal distance to the UAV, the UAV height above ground, and whether or not there is a LoS obstruction between the two (from the building topology map available to the UAV). Providing this trained neural network with the BS distances and channel types in the known area  $\mathcal{W}$  will allow REQIBA to estimate the total received interference power when the antenna is aligned with the given candidate BS, which it can then pass on to the DDQN for candidate BS selection.

This IPNN circuit consists of an input layer, two dense layers, and an output layer. The dense layers have 20 neurons each, with linear and tanh regularisation functions. The input consists of the matrices  $\mathbf{F}_\zeta$  and  $\mathbf{L}_\zeta$  and UAV height  $\gamma$ . The

output consists of a matrix of estimated signal power values for each of the corresponding interfering BSs. We sum the rows of this matrix to give the final output vector  $\mathbf{i}_\zeta = (n_1^t, n_2^t, \dots, n_\zeta^t)$ , where  $n_i^t$  is the estimated total interference power in the area  $\mathcal{W}_i$  that would be experienced by the UAV if it chooses the  $i$ -th candidate BS at timestep  $t$ .

2) *Dueling Deep Q Network*: Having estimated the interference power for each of the candidate BSs, and knowing their received signal powers and the current UAV association already, we propose a DDQN module to make the decision about which candidate BS to associate with for the current timestep. The DDQN module is based on model-free RL. In RL, the UAV chooses an action based on the observed environmental state at each timestep, based on what it expects will maximise the long-term reward. In a classic RL problem a so-called Q-Table is used, which maps the value of each possible action for a given environment state. As the UAV takes actions, the RL algorithm will observe the resulting action rewards and update the Q-Table accordingly. The Q-Table approach has been shown to be very effective for simple environments and action spaces, but if the environment is very large (and not easily discretised) then the Q-Table becomes very large and difficult to train. The solution to this is to apply a neural network to approximate the function of the Q-Table, that is, return the estimated Q-values of all possible actions for a given state. We apply a DDQN architecture to perform the function of this Q-Table, as shown in Fig. 4.

The DDQN takes the inputs  $\mathbf{p}_\zeta$ ,  $\mathbf{o}_\zeta$ ,  $\gamma$  and  $\mathbf{t}$  from the system input and  $\mathbf{i}_\zeta$  from the IPNN. The Q-value of a state-action pair is the sum of the state value and the action advantage functions; a typical Deep Q-Network (DQN) estimates the Q-value directly, whereas a DDQN contains two parallel streams which estimate the state value and the action advantage functions separately, before combining them together to form the Q-value [30]. This architecture has been shown to improve the policy evaluation of the neural network compared to the basic DQN architecture. The DDQN consists of an input layer, followed by a dense layer, followed by a split into two streams. In each stream there are two dense layers. The outputs of the streams are then passed into a combination layer where they are joined together to give  $\zeta$  Q-values, one for each possible action (candidate BS) for the given state. The output of this DDQN is a vector of the Q-values, with the action that has the largest Q-value being selected for the given timestep. Note that we do not explicitly provide any information to the DDQN about the handover penalty  $\tau$ ; the negative impact of handovers is to be learned by the DDQN over the course of its training, which will enable it to infer the cost of a handover in its decision process.

## V. TRAINING & EVALUATION METHODOLOGY

The environment described in Section III is simulated in the R programming language, using the "Keras" library for the REQIBA solution [31]. The environmental parameters of the simulated environment are given in Table I, and the REQIBA hyperparameters are given in Table II.

Before we can evaluate our REQIBA solution it needs to be trained. As REQIBA consists of two separate modules it

TABLE I  
NUMERICAL RESULT PARAMETERS

Parameter	Value
Carrier Freq	2 GHz
Simulation Area	5 km x 5 km
Building density $\beta$	300 /km <sup>2</sup>
Building land coverage $\delta$	0.5
Building height scale parameter $\kappa$	20 m
UAV velocity	10 m/s
LoS pathloss exponent $\alpha_L$	2.1
NLoS pathloss exponent $\alpha_N$	4
BS transmit power $p$	40 W
Near-field pathloss $c$	-38.4 dB [32]
Number of BS antenna elements $N_t$	8
Noise power $\sigma^2$	$8 \cdot 10^{-13}$ W [32]
Handover penalty factor $\tau$	0.5
BS height above ground $\gamma_G$	30 m
BS density $\lambda$	5 /km <sup>2</sup>
UAV height $\gamma$	100 m
UAV antenna beamwidth $\omega$	45 deg
MC trials	2000
Episodes per MC trial	1
Timesteps per episode T	100
Timestep duration	1 second

TABLE II  
REQIBA SOLUTION HYPERPARAMETERS

Parameter	Value
Q-value discount factor	0.1
Initial epsilon value $\epsilon$	1
Epsilon decay value	0.995
Minimum epsilon value	0.001
Replay memory size	10000 entries
Replay batch size	2048
Candidate BS number $\zeta$	10
Interfering BS number $\xi$	125

is trained in two stages, which we refer to as offline training and online training. The offline training involves training the IPNN. As this module is a regression neural network, it relies on supervised learning, wherein labelled data is presented to the network and it learns the relationship between the input and the output (the label). For our scenario this corresponds to the IPNN being presented with a dataset of interfering BS distances, channel types, UAV heights and the resulting received signal powers of those BSs. In a real-world scenario, this dataset would be generated by having the UAV fly around an urban environment and measure BS signal powers with its directional antenna, while also recording its horizontal distance and channel type. We simulate the generation of this dataset by simulating the urban environment over a number of Monte Carlo (MC) trials, with the UAV positioned at the centerpoint of the environment. In each trial the UAV points its directional antenna towards a random BS and records the signal power observed by the directional antenna, alongside the horizontal distance to the BS, its channel type (based on the known building topology) and the height of the UAV. These measurements populate a dataset which is then used to train the IPNN.

Having trained the IPNN, we carry out the online training of the DDQN. We refer to it as online training, as the DDQN is trained during the normal operation of the UAV, in the typical manner of RL. We again simulate a number of MC trials with generated urban environments and UAV



travel trajectories. For each MC trial the UAV moves from the start to the end-point in a straight line over  $T$  timesteps. At each timestep REQIBA takes the state inputs, generates the aggregate interference powers via the IPNN, then estimates the Q-values via the DDQN. We follow an  $\epsilon$ -greedy training procedure, following which a candidate BS is chosen either at random with probability  $\epsilon$  or based on the highest Q-value as estimated by the DDQN with probability  $1 - \epsilon$ . The reward (timestep throughput  $\rho^t$ ) is observed. The state inputs, the action taken, the reward, and the next state inputs are stored in a so-called replay buffer. Once this replay buffer has a sufficient number of entries it is used to train the DDQN, via uniform sampling of the replay buffer into batches of training data. The value of  $\epsilon$  is decayed by a certain factor at the end of each step, so the training process will randomly explore the environment in the beginning and then rely less and less on random decisions as the DDQN becomes more and more trained.

We propose evaluating our REQIBA solution in two stages. In the first stage we compare the performance of REQIBA to the BS association solution in our prior work [9]. While this prior solution is designed for a static scenario, it can be applied to a mobile scenario as well. By taking this prior solution as a baseline we quantify the performance gains that REQIBA can provide. REQIBA is composed of the IPNN and DDQN modules which process parts of the state inputs, and both of these modules can be used to make a BS association decision in isolation of one another. To verify the performance benefits of the full REQIBA solution we compare it against the performance of the IPNN and DDQN modules in isolation.

In the second evaluation stage we verify the performance of REQIBA against heuristic BS association schemes. As the UAV has access to important information about the environment it is capable of making BS association decisions by following simple heuristic schemes. In our prior work [9] we demonstrated that the performance improvement from applying ML is highly dependent on the environmental conditions, and that under certain circumstances the simple heuristic association schemes may be sufficient for the UAV. For this reason, we are interested in comparing how REQIBA performs against heuristics under various environmental conditions. This will give us valuable insight on how the environment can determine the most appropriate type of association policy.

## VI. EVALUATION RESULTS AGAINST PRIOR MODEL

In this section we compare the performance of the two REQIBA modules, the IPNN and the DDQN, against the performance of our prior static model from [9]. The purpose of this comparison is two-fold. First, we verify that the REQIBA solution offers a performance improvement over our prior solution, which does not make use of the IPNN and DDQN modules. Second, as REQIBA makes use of two connected modules to make an association decision, we verify that both modules offer measurable performance benefits when working together, to validate our choice of solution. We consider two performance metrics for our comparison: the total throughput over an entire episode, and the handover rate

over an episode. This performance comparison is carried out across a range of UAV heights. For ease of comparison of the episode throughput, we take the total episode throughput of our prior solution as a baseline, and normalise the total episode throughput of the IPNN and DDQN modules with respect to it. For this comparison we consider three variants of the DDQN module: The results labelled "IPNN+DDQN" use the full REQIBA solution as described in Section IV; the results labelled "DDQN (No Int.)" are for the DDQN module acting in isolation with no inputs relating to the interference power; and the results "DDQN (With Int.)" are for the DDQN acting in isolation and taking in the matrices  $\mathbf{F}_\zeta$  and  $\mathbf{L}_\zeta$  directly. Finally, the results labelled "IPNN" show the performance when an association decision is made by choosing the BS with the lowest interference power in  $\mathbf{i}_\zeta$  as estimated by the IPNN, without involving the DDQN.

Fig. 5 shows the resulting throughput performance, and Fig. 6 the handover rates. We note that REQIBA improves the episode throughput by as much as 50% when compared to the baseline, while offering a significant reduction in the handover rate. This is because REQIBA offers several improvements over the prior solution. First, the dedicated IPNN module is better at estimating the expected interference power than the prior solution, which makes REQIBA more reliable in its candidate BS selection. Second, REQIBA is able to explicitly learn the negative impact of handovers and take that into consideration by means of its DDQN module, whereas the prior solution is designed for a static UAV scenario, and so ignores the impact of handovers. This causes the prior solution to make an excessive amount of handovers during UAV flight, which negatively impacts the episode throughput. This behaviour suggests that the mobile UAV connectivity problem cannot be adequately solved by treating it as a sequence of independent static decisions, as the prior solution does.

Comparing the performance of the two modules we see that it is heavily determined by the UAV height. The IPNN in isolation gives very similar throughput improvement as the joint IPNN+DDQN solution at greater heights, although it performs worse than the baseline at low heights. We explain these observations by the effect of interference at different heights. At low heights interference power is low and the association decision is primarily down to the received signal power from the BSs, which makes the IPNN block unnecessary for the decision-making. This results in the IPNN+DDQN solution performing very similar to the baseline. As the height increases the interference starts to play more and more of a role, and so does the IPNN module. As a result of this the solutions which use the IPNN module give an improvement over the baseline. Note that the baseline solution is capable of inferring some information about interference (albeit not as well as the dedicated IPNN module) and so it ends up outperforming the DDQN module when the latter is not connected to the IPNN. It is interesting to note that passing information about the interfering BSs directly to the DDQN does not improve its performance when compared to not passing it that information; it appears that the DDQN is not capable of learning to directly interpret the interference power from the BS distances and

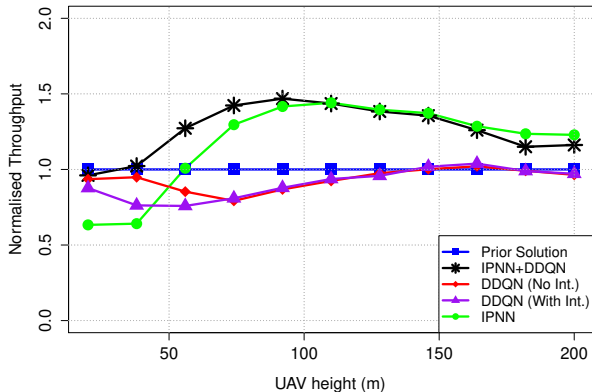


Fig. 5. Normalised throughput showing the performance of the IPNN and DDQN modules against our prior solution, at different UAV heights.

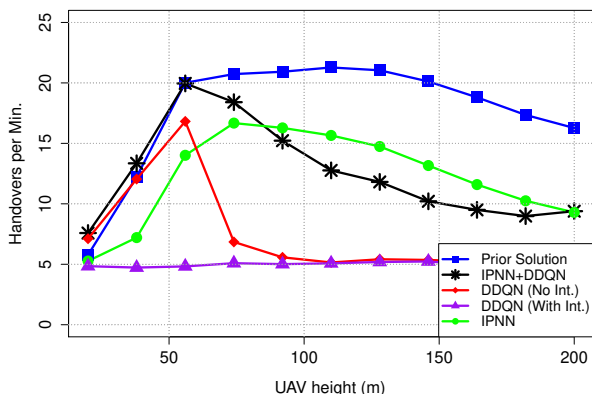


Fig. 6. Handover rate showing the performance of the IPNN and DDQN modules against our prior solution, at different UAV heights.

channel types, and needs the IPNN module to perform this function. While the DDQN may not be able to provide a good episode throughput without the help of the IPNN, it still plays an important role in managing the rate of handovers, as we demonstrate in Fig. 6. We observe how the IPNN+DDQN solution is able to achieve a lower handover rate at greater heights than the pure IPNN solution, while still managing a very similar throughput. This demonstrates that while the IPNN module by itself may be sufficient for maximising the episode throughput when the UAV is operating in certain interference-heavy conditions, the DDQN module is needed to reduce the resulting rate of handovers. We explore this behaviour further in the next section.

## VII. EVALUATION RESULTS AGAINST HEURISTIC ASSOCIATION

Having verified that our proposed REQIBA solution provides a significant performance boost over our prior solution, we now evaluate how well REQIBA compares against heuristic association schemes under different environmental conditions. As the problem of UAV association and handover is new, there is no established performance benchmark to compare against; we therefore perform a comparison against common heuristic solutions. As we observed in the previous section, the IPNN module by itself can provide good performance under some

circumstances, which is why we include it alongside the full IPNN+DDQN solution in the following results. The heuristic algorithms selected in this section are detailed below:

- **Closest BS association.** As the UAV has a map of the BSs, it can determine which BS is the closest to it at any given timestep. Under this association scheme the UAV always connects to the closest BS, regardless of the received signal powers or current association. This association is depicted in blue in the figures below.
- **Highest SINR association.** The omni-directional antenna on the UAV can measure the SINR of the channel for the strongest signal BSs around it. While this omni-directional SINR will differ to the SINR of the directional antenna when aligned, it can still be used to make an association decision directly, instead of using the REQIBA modules. This type of association corresponds to the usual association policy used by ground users. This association is depicted in red.
- **Shortest mean distance association.** We have assumed in our scenario that the UAV does not know its trajectory and where it will be in future timesteps. For the sake of a heuristic comparison, we relax this assumption. If the UAV knows its trajectory over the whole episode, it can choose to connect to the BS which has the shortest average distance to the UAV across all timesteps. This association is depicted in orange.
- **Angle alignment association.** If the UAV knows the locations of the BSs and it knows its own trajectory, it is aware of the BS whose direction is the closest to the direction that the UAV is travelling in. To represent a scenario where realigning the directional antenna may be undesirable, we consider an association scheme where the UAV associates with the BS which is the best-aligned with the direction of the UAV flight. This association is depicted in purple.

Unless stated otherwise the results in the figures below are based on the values in Tables I and II. In the following subsections we vary the UAV height, BS density, building density, UAV antenna beamwidth, and handover penalty, and report on the comparative performance of REQIBA against the other association schemes. As in the previous section, we normalise the episode throughput of the different association schemes with respect to a baseline, which in this section corresponds to the episode throughput achieved from the closest association scheme.

### A. UAV Height

In Fig. 7 we show the normalised throughput achieved for the different association schemes under varying UAV heights. We note that the IPNN+DDQN association scheme outperforms all of the heuristics across the entire range of heights, giving as much as a 70% throughput improvement over the best heuristic scheme. As in Fig. 5, the IPNN association scheme gives poor performance at low heights where interference power is low, and gives good performance at large heights, slightly improving on the IPNN+DDQN scheme. At low heights the BS antenna sidelobe gain plays an important



role in the signal performance. As a result, the IPNN+DDQN association scheme, which takes into account several factors such as interference, antenna gain, and BS load, is able to outperform any other association scheme which only considers one factor, while the IPNN association scheme performs worse than the simple SINR heuristic, despite making use of a trained neural network. At large heights, however, the dominating factor is interference, and choosing a BS exclusively based on the resulting interference gives the best throughput.

When we consider handover, the SINR association heuristic results in extremely large handover rates, while the remaining heuristics have either no handovers or very few, as expected. The REQIBA-based association schemes fall in-between the two extremes; on the one hand, they are able to make better decisions than the SINR association and so do not carry out handovers as often, but on the other hand the fact that they are very dynamic in responding to the changing radio environment means that they still result in a much higher handover rate than the closest BS association scheme. Considering that at very large heights the REQIBA-based schemes offer a relatively modest throughput improvement (approximately 20%) over the closest BS association, this significant increase in handover rates may not be justified, in which case it may be worthwhile for the UAV to rely on simple closest BS association.

It is also worth noting that the mean distance-based association and angle-aligned association give relatively poor throughput performance, despite benefiting from *a priori* knowledge of the UAV travel path, which the other association schemes are assumed not to know. The advantage of these association schemes is that they allow the UAV to pick a single BS to connect to and maintain that connection for the entire episode, and so these associations may be useful where limiting the number of handovers is more important than obtaining high throughput.

### B. BS Density

Fig. 9 shows the impact of the BS density  $\lambda$  on the normalised throughput. At lower densities the IPNN+DDQN association scheme gives significant improvements over all of the other association schemes, although as the density

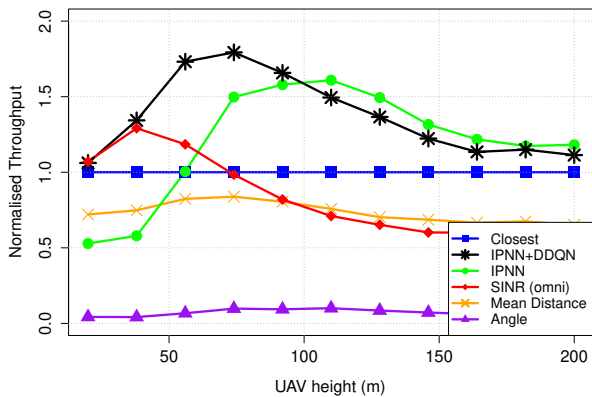


Fig. 7. Normalised throughput showing the performance of our REQIBA modules, as well as the heuristics, for different UAV heights.

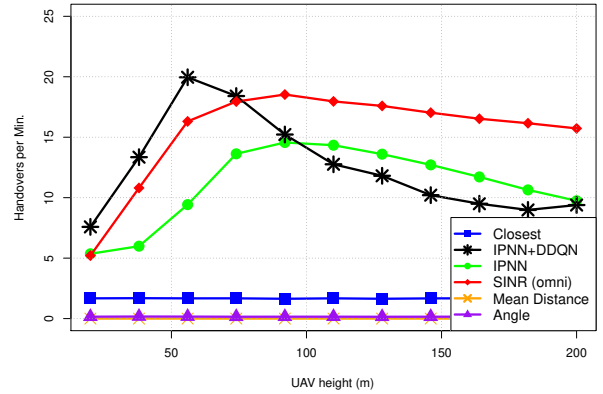


Fig. 8. Handover rate showing the performance of our REQIBA modules, as well as the heuristics, for different UAV heights.

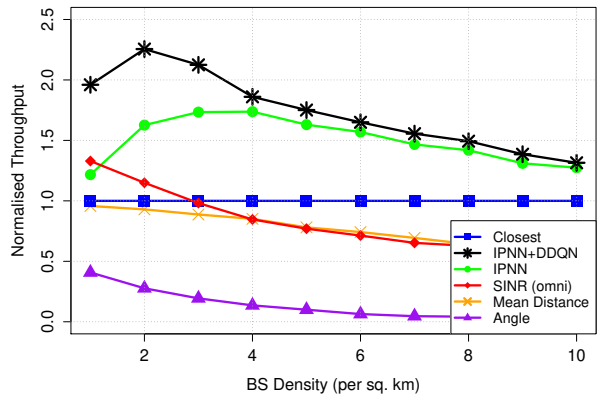


Fig. 9. Normalised Throughput showing the performance of our REQIBA modules, as well as the heuristics, for different BS densities.

increases the performance appears to converge to that of the IPNN association scheme. This reinforces our observations in the previous sub-section: at low densities a number of factors determine which of the candidate BSs the UAV should connect to, whereas as the density increases the interference power becomes the primary deciding factor, which renders the IPNN+DDQN association marginally better than the IPNN association, in terms of throughput. As before, the handover rates in Fig. 10 show that the IPNN+DDQN solution improves throughput at the expense of a large handover rate, and that increasing the amount of interference in the environment will result in the IPNN+DDQN providing a reduced handover rate compared to the pure IPNN-based association scheme.

### C. Building Density

Fig. 11 and Fig. 12 show the performance under different densities of buildings in the urban environment. Increasing the building density leads to more LoS blocking obstacles in the environment, which results in wireless channels that fluctuate significantly more as the UAV moves. The IPNN module, as it only considers aggregate interference power, struggles to adapt to this dynamism and so the normalised throughput degrades with increasing density. The IPNN+DDQN solution is aware of both interference powers as well as candidate BS powers, so it is capable of adapting to this increasing channel

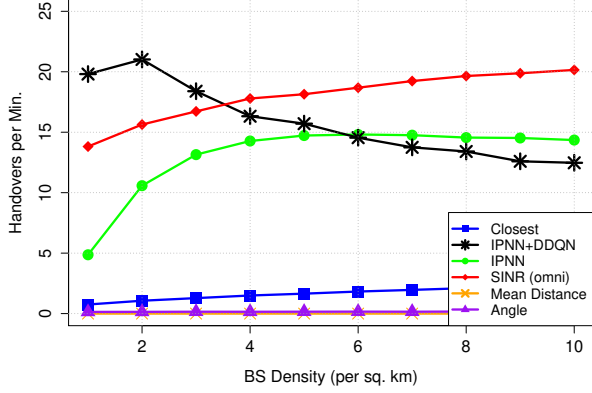


Fig. 10. Handover rate showing the performance of our REQIBA modules, as well as the heuristics, for different BS densities.

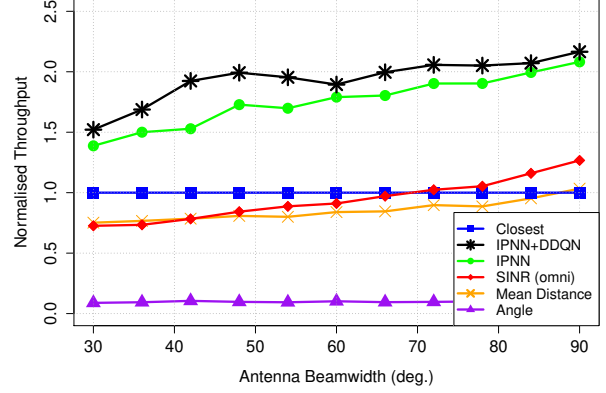


Fig. 13. Normalised Throughput showing the performance of our REQIBA modules, as well as the heuristics, for different UAV antenna beamwidths.

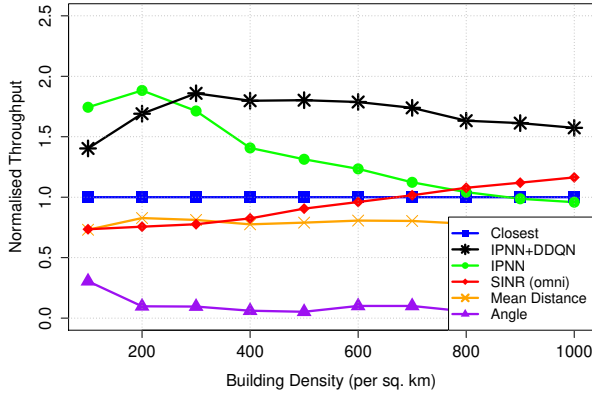


Fig. 11. Normalised Throughput showing the performance of our REQIBA modules, as well as the heuristics, for different building densities.

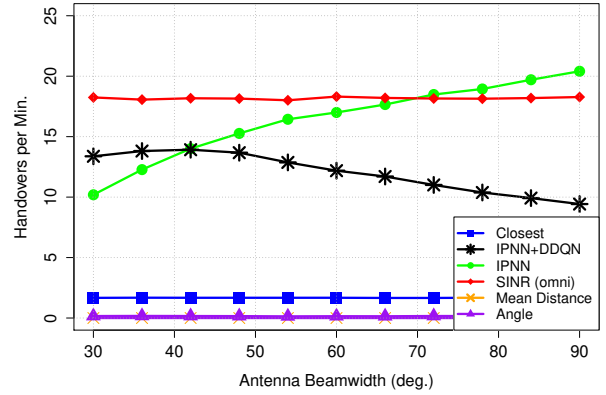


Fig. 14. Handover rate showing the performance of our REQIBA modules, as well as the heuristics, for different UAV antenna beamwidths.

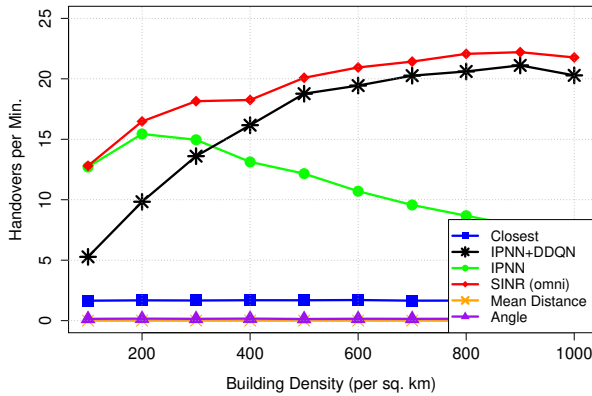


Fig. 12. Handover rate showing the performance of our REQIBA modules, as well as the heuristics, for different building densities.

complexity, and manages to maintain a relatively stable performance improvement over the baseline. As a consequence of reacting to the increasingly dynamic radio environment the IPNN+DDQN solution sees an increase in the handover rate as the building density increases. We note that very densely built-up environments require very frequent handovers to respond to the volatile radio conditions.

#### D. UAV Beamwidth

Fig. 13 and Fig. 14 show the effects of UAV antenna beamwidth on the performance. Increasing the beamwidth of the antenna allows more interfering BSs to be illuminated by the directional antenna, which increases the overall interference power. The result of this is that it appears to increase the fluctuations in interference power, as Fig. 14 shows a significant increase in the handover rate of the IPNN-based association scheme. By contrast, the DDQN association scheme is able to recognise the negative impact of these interference fluctuations and is able to intelligently avoid unnecessary handovers, thus reducing the handover rate as the beamwidth increases. It is interesting to note that the resulting normalised throughput appears to be quite similar for both REQIBA-based association schemes, as the IPNN scheme focuses on improving the channel quality at all costs, while the IPNN+DDQN may opt for a worse channel, but benefit from the reduced overheads of frequent handovers.

#### E. Handover Penalty

We now consider the effect of the handover penalty  $\tau$  on the UAV performance. Recall that  $\tau$  has a range between 0 and 1, and impacts the received reward in a timestep where a handover occurs. Values of  $\tau$  closer to 0 correspond to heavy

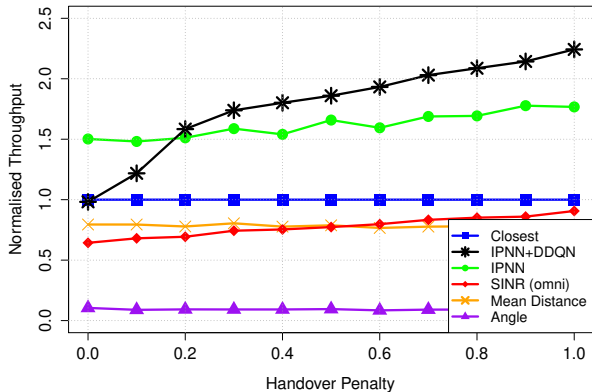


Fig. 15. Normalised Throughput showing the performance of our REQIBA modules, as well as the heuristics, for different handover penalty factors  $\tau$ .

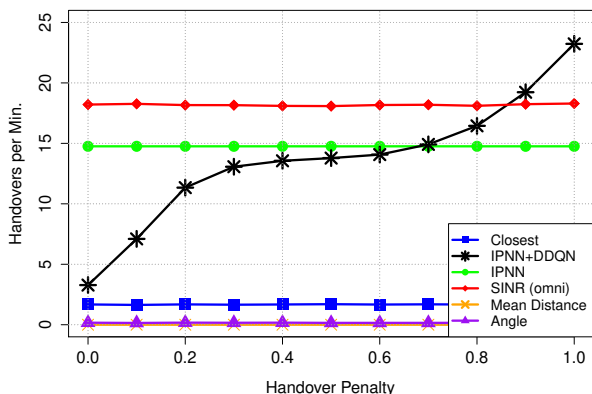


Fig. 16. Handover rate showing the performance of our REQIBA modules, as well as the heuristics, for different handover penalty factors  $\tau$ .

penalty for carrying out a handover, and this is reflected in the resulting throughput shown in Fig. 15. The figure shows that the IPNN+DDQN based association method suffers heavily for low values of  $\tau$ . The DDQN module relies on trial-and-error exploration to learn which actions to take for a given observed state; low values of  $\tau$ , however, heavily punish any exploration and attempts to connect to better BSs. This causes the DDQN module to learn a very conservative association policy which results in very low throughput performance, much lower than the IPNN association scheme, which ignores the impact of handover penalties entirely. It is worth noting that the IPNN scheme appears to only suffer minor throughput degradation for lower values of  $\tau$ , despite the relatively large handover rate, as shown in Fig. 16. We can see that for low values of  $\tau$  the IPNN+DDQN solution prioritises minimising the handover rate at all costs, while as  $\tau$  increases the IPNN+DDQN association scheme begins to more freely carry out handovers during flight, even exceeding the handover rate of the IPNN-based association above a certain point.

## VIII. DISCUSSION & CONCLUSION

In this paper we have proposed an ML-based BS association scheme referred to as REQIBA that would allow a UAV moving through an urban area to intelligently choose which BSs to connect to, to maximise the overall data throughput

during the flight while keeping the rate of handovers manageable. Our proposed solution consisted of two modules: a regression neural network module for estimating the aggregate interference powers for each candidate BS's channel, and a DDQN module for choosing the candidate BS in each timestep, based on RL training. Our numerical results show that the REQIBA solution allows a UAV to significantly improve its total throughput, when compared to the ML solution we proposed for a static UAV scenario in our prior work [9], as well as to heuristic association schemes that use the available environment information. It has been established by the wireless community that UAV wireless channels are interference-limited due to the lack of signal blockage; we have shown that under certain conditions the interference power is such an issue that we can achieve the best throughput by simply choosing the candidate BS with the lowest interference power on its channel, without taking into account other factors such as the signal power of the candidate BSs or the effects of handovers. The use of our full REQIBA solution with the DDQN module becomes justified when the environment is less influenced by interference (such as due to lower BS density or lower UAV height above ground), and where achieving the best throughput means balancing a number of environmental factors in the decision process. Even in scenarios where the IPNN module alone is sufficient to maximise the throughput, the DDQN module plays an important role in managing the rate of handovers, as it explicitly factors in the impact of carrying out a handover to a new BS. Without this function, the UAV may carry out very frequent handovers to respond to the dynamic environmental conditions, in the order of one handover every three or four seconds according to our results.

Our analysis shows that while the REQIBA solution using the joint IPNN+DDQN association can offer significant benefits to the UAV, there are certain important caveats that need to be taken into account by the UAV operators before choosing it for the BS association task. First of all, we have demonstrated that interference power prediction is a mandatory phase of the association decision process; while the IPNN module could be used in isolation to make association decisions, the DDQN module relies on information about the interference power, and cannot provide good performance without this input. The DDQN module was also shown to react negatively to strong handover penalties, as the penalty punishes any exploration carried out by the DDQN, which causes the training process to learn to pursue a handover-minimisation scheme, giving relatively poor results. By comparison, the simpler IPNN-only association scheme was shown to be much more resilient to strong handover penalties, and would be a more appropriate scheme to use in situations where the handover penalties are severe.

Ultimately, the problem of mobility management involves finding a balance between maximising the channel quality of a moving device while minimising the cost incurred by handovers. Allowing a device the flexibility of choosing its associated BS with the changing environment carries the cost of more frequent handovers. If the overheads associated with the handovers are too great, or if the UAV use-case requires low handover rates, then an ML-based association scheme may

not be the most appropriate choice in some circumstances. Our results have shown that while certain heuristic association schemes (such as the highest-SINR association scheme) are wholly inappropriate for UAV connectivity, other schemes (such as closest BS association) can offer very low handover rates, and therefore may be the most suitable association schemes to adopt in some scenarios.

In this work we have considered optimising the downlink channel of a cellular-connected UAV. In future works we may consider the uplink channel instead, which would necessitate taking into account the behaviour of ground users also being served by the BS network. In this work we have also assumed that all BSs have the same bandwidth resources available for the UAV; in future works we may relax this assumption and consider an ML-based association scheme which intelligently chooses BS associations not only based on wireless channel quality and handover costs, but also based on available spectrum resources.

#### ACKNOWLEDGEMENT

This material is based upon works supported by the Science Foundation Ireland under Grants No. 17/NSFC/5224 and 13/RC/2077.

#### REFERENCES

- [1] CNN, "First Drone Delivery of a Donated Kidney Ends with Successful Transplant," May 2019. [Online]. Available: <https://edition.cnn.com/2019/05/01/health/drone-organ-transplant-bn-trnd/index.html>
- [2] M. Mozaffari, W. Saad, M. Bennis, Y. Nam, and M. Debbah, "A Tutorial on UAVs for Wireless Networks: Applications, Challenges, and Open Problems," *IEEE Communications Surveys & Tutorials*, vol. 21, no. 3, pp. 2334–2360, Third Quarter 2019.
- [3] "TR 36.777: Technical Specification Group Radio Access Network; Study on Enhanced LTE Support for Aerial Vehicles (Release 15)," 3GPP, Tech. Rep., 2018.
- [4] R. Amer, W. Saad, and N. Marchetti, "Mobility in the Sky: Performance and Mobility Analysis for Cellular-Connected UAVs," *IEEE Transactions on Communications*, vol. 68, no. 5, pp. 3229 – 3246, May 2020.
- [5] R. Amer, W. Saad, and N. Marchetti, "Toward a Connected Sky: Performance of Beamforming With Down-Tilted Antennas for Ground and UAV User Co-Existence," *IEEE Communications Letters*, vol. 23, no. 10, pp. 1840–1844, Oct. 2019.
- [6] X. Ge, "Ultra-Reliable Low-Latency Communications in Autonomous Vehicular Networks," *IEEE Transactions on Vehicular Technology*, vol. 68, no. 5, pp. 5005–5016, May 2019.
- [7] X. Lin *et al.*, "The Sky Is Not the Limit: LTE for Unmanned Aerial Vehicles," *IEEE Communications Magazine*, vol. 56, no. 4, pp. 204–210, April 2018.
- [8] "TR 36.777 Annex H : Field Trials Results on Mobility," 3GPP, Tech. Rep., 2018.
- [9] B. Galkin, R. Amer, E. Fonseca, and L. A. DaSilva, "Intelligent Base Station Association for UAV Cellular Users: A Supervised Learning Approach," in *IEEE 5G World Forum*, Sept. 2020.
- [10] "LTE Unmanned Aircraft Systems," Qualcomm Technologies, Inc, Tech. Rep., 2017.
- [11] M. M. Azari, F. Rosas, and S. Pollin, "Cellular Connectivity for UAVs: Network Modeling, Performance Analysis and Design Guidelines," *IEEE Transactions on Wireless Communications*, vol. 18, no. 7, pp. 3366–3381, July 2019.
- [12] J. Stanczak, I. Z. Kovacs, D. Koziol, J. Wigard, R. Amorim, and H. Nguyen, "Mobility Challenges for Unmanned Aerial Vehicles Connected to Cellular LTE Networks," in *IEEE Vehicular Technology Conference (VTC Spring)*, June 2018.
- [13] S. Euler, H. Maattanen, X. Lin, Z. Zou, M. Bergström, and J. Sedin, "Mobility Support for Cellular Connected Unmanned Aerial Vehicles: Performance and Analysis," in *IEEE Wireless Communications and Networking Conference (WCNC)*, April 2019.
- [14] A. Fakhreddine, C. Bettstetter, S. Hayat, R. Muzaffar, and D. Emini, "Handover Challenges for Cellular-Connected Drones," in *Proc. of ACM Workshop on Micro Aerial Vehicle Networks, Systems, and Applications*, June 2019, pp. 9–14.
- [15] R. Amer, W. Saad, B. Galkin, and N. Marchetti, "Performance Analysis of Mobile Cellular-Connected Drones under Practical Antenna Configurations," in *IEEE International Conference on Communications (ICC)*, June 2020.
- [16] S. Zhang, Y. Zeng, and R. Zhang, "Cellular-Enabled UAV Communication: A Connectivity-Constrained Trajectory Optimization Perspective," *IEEE Transactions on Communications*, vol. 67, no. 3, pp. 2580–2604, March 2019.
- [17] J. Chen and D. Gesbert, "Optimal Positioning of Flying Relays for Wireless Networks: A LOS Map Approach," in *IEEE International Conference on Communications (ICC)*, May 2017.
- [18] O. Esrafilian and D. Gesbert, "Simultaneous User Association and Placement in Multi-UAV Enabled Wireless Networks," in *ITG Workshop on Smart Antennas (WSA)*, March 2018.
- [19] R. Gangula, D. Gesbert, D. F. Külzer, and J. M. Franceschi, "A Landing Spot Approach for Enhancing the Performance of UAV-Aided Wireless Networks," in *IEEE International Conference on Communications Workshops (ICC Workshops)*, May 2018.
- [20] U. Challita, W. Saad, and C. Bettstetter, "Deep Reinforcement Learning for Interference-aware Path Planning of Cellular-Connected UAVs," in *IEEE International Conference on Communications (ICC)*, May 2018.
- [21] Y. Zeng and X. Xu, "Path Design for Cellular-Connected UAV with Reinforcement Learning," in *IEEE Global Communications Conference (GLOBECOM)*, Dec. 2019.
- [22] X. Zhong, Y. Huo, X. Dong, and Z. Liang, "Deep Q-Network Based Dynamic Movement Strategy in a UAV-Assisted Network," *Arxiv e-prints*, Aug. 2020.
- [23] M. M. U. Chowdhury, W. Saad, and I. Guvenc, "Mobility Management for Cellular-Connected UAVs: A Learning-Based Approach," *Arxiv e-prints*, Feb. 2020.
- [24] A. Azari, F. Ghavimi, M. Ozger, R. Jantti, and C. Cavdar, "Machine Learning Assisted Handover and Resource Management for Cellular Connected Drones," in *IEEE Vehicular Technology Conference (VTC Spring)*, May 2020.
- [25] Y. Chen, X. Lin, T. A. Khan, and M. Mozaffari, "A Deep Reinforcement Learning Approach to Efficient Drone Mobility Support," *Arxiv e-prints*, May 2020.
- [26] A. Takács, R. Manghirmalani, H. Mahkonen, Y.-P. E. Wang, and L. Xingqin, "Methods and Systems for Using an Unmanned Aerial Vehicle (UAV) Flight Path to Coordinate an Enhanced Handover in 3rd Generation Partnership Project (3GPP) Networks," Apr. 16 2020, US Patent App. 16/610,049.
- [27] B. Galkin, J. Kibilda, and L. A. DaSilva, "Backhaul for Low-Altitude UAVs in Urban Environments," in *IEEE International Conference on Communications (ICC)*, May 2018.
- [28] "Recommendation P.1410-5 "Propagation Data and Prediction Methods Required for the Design of Terrestrial Broadband Radio Access Systems Operating in a Frequency Range From 3 to 60 GHz"," ITU-R, Tech. Rep., 2012.
- [29] X. Xu and Y. Zeng, "Cellular-Connected UAV: Performance Analysis with 3D Antenna Modelling," in *IEEE International Conference on Communications Workshops (ICC Workshops)*, May 2019.
- [30] Z. Wang, T. Schaul, M. Hessel, H. Hasselt, M. Lanctot, and N. Freitas, "Dueling Network Architectures for Deep Reinforcement Learning," in *International Conference on Machine Learning*, June 2016, pp. 1995–2003.
- [31] "R Interface to Keras." [Online]. Available: <https://keras.rstudio.com/>
- [32] H. Elshaer, M. N. Kulkarni, F. Boccardi, J. G. Andrews, and M. Dohler, "Downlink and Uplink Cell Association With Traditional Macrocells and Millimeter Wave Small Cells," *IEEE Transactions on Wireless Communications*, vol. 15, no. 9, pp. 6244–6258, Sept. 2016.